Dalton Transactions

Cite this: *Dalton Trans.*, 2012, **41**, 8941

www.rsc.org/dalton

PAPER

Synthesis, characterization and some properties of mononuclear Ni and trinuclear $NiFe_2$ complexes related to the active site of [NiFe]-hydrogenases†

Li-Cheng Song,* Xiao-Jing Sun, Pei-Hua Zhao, Jia-Peng Li and Hai-Bin Song

Received 17th March 2012, Accepted 21st May 2012
DOI: 10.1039/c2dt30609c

The $[N_2S_2]$-type ligand 1,2-(2-$C_5H_4NCH_2S)_2C_6H_4$ (**L**) is prepared in 84% yield by a new method and its structure has been confirmed by X-ray crystallography. The new synthetic method involves sequential reaction of 1,2-phenylenedithiol with EtONa followed by treatment of the resulting disodium salt of 1,2-phenylenedithiol with *in situ* generated 2-(chloromethyl)pyridine from its HCl salt. Further treatment of ligand **L** with $NiCl_2·6H_2O$ or NiI_2 affords the expected new mononuclear Ni complexes Ni[1,2-(2-$C_5H_4NCH_2S)_2C_6H_4$]Cl_2 (**1**) and Ni[1,2-(2-$C_5H_4NCH_2S)_2C_6H_4$]I_2 (**3**) in 87–88% yields, whereas reaction of **L** with $NiBr_2$ under similar conditions results in formation of the expected new mononuclear complex Ni[1,2-(2-$C_5H_4NCH_2S)_2C_6H_4$]Br_2 (**2**) and one unexpected new mononuclear complex Ni[1-(2-$C_5H_4NCH_2S$)-2-(2-$C_5H_4NCH_2SC_6H_4S$)C_6H_4]Br_2 (**2***) in 82% and 5% yields, respectively. More interestingly, the ligand **L**-containing novel trinuclear $NiFe_2$ complex Ni{[1,2-(2-$C_5H_4NCH_2S)_2C_6H_4$}$Fe_2(CO)_6(\mu_3\text{-}S)_2$ (**4**) is found to be prepared by sequential reaction of (μ-S_2)$Fe_2(CO)_6$ with Et_3BHLi, followed by treatment of the resulting (μ-LiS)$_2Fe_2(CO)_6$ with mononuclear complex **1**, **2**, or **3** in 12–20% yields. The new complexes **1–4** and **2*** are fully characterized by elemental analysis and various spectroscopies, and the crystal structures of **1**, **2*** and **3** as well as some electrochemical properties of **1–4** are also reported.

Introduction

Hydrogenases are natural enzymes that can catalyze the reversible redox reaction between molecular hydrogen and protons in many microorganisms.[1–4] These enzymes can be classified into three major groups according to the metal content in their active sites, namely [FeFe]-hydrogenases ([FeFe]Hases),[5–7] [NiFe]-hydrogenases ([NiFe]Hases),[8–10] and iron–sulfur cluster-free hydrogenase (Hmd).[11–13] The X-ray structure determination for [NiFe]Hases isolated from *Desulfovibrio* (*D.*) *gigas*,[14] *D. vulgaris* Miyazaki F,[15] and *Desulfomicrobium* (*Dm.*) *baculatum*[16] revealed that they have two forms of active sites. One is the oxidized form, whose Ni and Fe atoms are bridged by two cysteine S atoms and one O atom with a Ni–Fe distance of 2.5–2.9 Å. The other reduced form has a Ni–Fe bond of 2.5–2.6 Å bridged by two cysteine S atoms or perhaps with an additional H-bridge. Although the crystal structures of the active sites of [NiFe]Hases have some differences, they have some interesting common features. That is, all the active sites of [NiFe]Hases consist of a butterfly $[NiFeS_2]$ cluster core in which the Fe atom is coordinated by one terminal CO and two terminal CN^- ligands, the Ni atom is coordinated by two terminal cysteine S (Cys–S) ligands (an exception is for *Dm. baculatum* in which its Ni atom is coordinated by one terminal Cys–S ligand and one terminal seleno–cysteine Se (Cys–Se) ligand), and the two metal centers are combined together by two bridging Cys–S ligands (Fig. 1).[14–18]

Under the guidance of the well-elucidated structures regarding the active sites of [NiFe]Hases, synthetic chemists have successfully prepared a great variety of mononuclear Ni or Fe complexes and heteronuclear Ni–Fe complexes as models for the active site of [NiFe]Hases.[19–21] Now, we wish to report our results on the synthesis, structural characterization and some properties of four new mononuclear Ni complexes and one novel trinuclear $NiFe_2$ cluster complex. Interestingly, these complexes, according to their metal centers and the surrounding heteroatom ligands, could be regarded as the structural analogues of the mononuclear Ni moiety and/or the dinuclear Ni/Fe moiety in the active site of [NiFe]Hases.

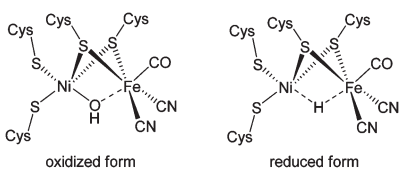

Fig. 1 Schematic structures of the active sites of [NiFe]Hases determined by protein X-ray crystallography.

Department of Chemistry, State Key Laboratory of Elemento-Organic Chemistry, Nankai University, Tianjin 300071, China. E-mail: lcsong@nankai.edu.cn

†Electronic supplementary information (ESI) available: Fig. S1–S32: the 1D-NMR spectra of **L**, **1**, **2**, **2***, **3**, and **4**; Fig. S33–S56: the 2D-NMR spectra of **L**, **2**, **2***, **3**, and **4**; Fig. S57–S60: the EPR spectra of **1**, **2***, **3**, and **4**. CCDC 871093–871096. For ESI and crystallographic data in CIF or other electronic format see DOI: 10.1039/c2dt30609c

Results and discussion

Synthesis and characterization of ligand 1,2-(2-$C_5H_4NCH_2S)_2$-C_6H_4 (L)

In order to synthesize the designed structural analogues of the active site of [NiFe]Hases reported in this article, we developed a new synthetic method for preparation of the $[N_2S_2]$-type ligand **L**. This new method, as shown in Scheme 1, involves a sequential reaction of 1,2-phenylenedithiol with 2 equiv of EtONa (formed *in situ* from sodium and EtOH) followed by treatment of the intermediate disodium salt of 1,2-phenylenedithiol with 2 equiv of 2-(chloromethyl)pyridine (generated *in situ* from 2 equiv of 2-(chloromethyl)pyridine hydrochloride and 2 equiv of EtONa), resulting in formation of ligand **L** in up to 84% yield. It is worth pointing out that the new method is different from the previously reported one[22] in two ways. Firstly, the new method is simply to use the *in situ* generated 2-(chloromethyl)-pyridine from commercially available 2-(chloromethyl)pyridine hydrochloride, whereas the previously reported one uses the pre-prepared 2-(chloromethyl)pyridine. Secondly, the new one uses a workup procedure including TLC separation followed by solidification and recrystallization to give a solid product in high purity (we have determined its crystal structure, see below), whereas the previously reported one utilizes a workup procedure including extraction followed by washing to obtain an oily product.

Ligand **L** is a yellowish and air-stable solid, which was fully characterized by elemental analysis, spectroscopy and notably by X-ray crystallography. For example, the C/H/N analytical data were in good agreement with its composition, whereas its IR spectrum showed two absorption bands at 1641 and 746 cm^{-1} for its C═N double bonds and C–S single bonds, respectively. In addition, the ^1H and ^{13}C NMR data of **L** were obtained by using two-dimensional NMR techniques, such as the ^1H-^1H COSY, ^1H-^1H NOESY, ^1H-^{13}C HMQC, and ^1H-^{13}C HMBC techniques (see the ESI†). In its ^1H NMR spectrum, the doublets at 7.29 and 8.53 ppm can be assigned to 3-H and 6-H in its pyridine rings, whereas the multiplets at 7.04–7.06 and 7.23–7.25 ppm can be ascribed to 4,5-H and 3,6-H in its benzene rings, respectively. In addition, in its ^{13}C NMR spectrum the signals at 122.1, 123.2, 136.6, 149.3, and 157.4 ppm can be ascribed to the five carbon atoms of C5, C3, C4, C6, and C2 in its pyridine rings, whereas the signals at 126.9 and 130.0 ppm can be attributed to the four carbon atoms of C4/C5 and C3/C6 in its benzene rings, respectively. The molecular structure of **L** determined by X-ray crystal diffraction techniques is shown in Fig. 2, and Table 1 lists the selected bond lengths and angles. As can be seen intuitively from Fig. 2, the two pyridine rings are indeed attached to the two ortho-carbon atoms of a benzene ring *via* two methylenethio groups. The two C–S–C bond angles are 103.64° and 105.05° respectively. The four C–S bond lengths vary from 1.770 to 1.813 Å. The dihedral angle between the two pyridine rings is 83.28°, whereas the two dihedral angles between each pyridine ring and the benzene ring are 76.63° and 82.81° respectively.

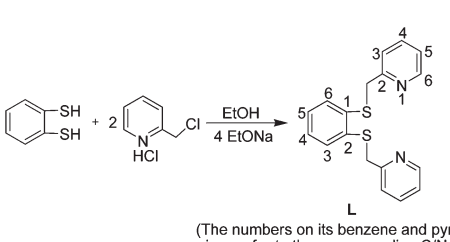

Scheme 1

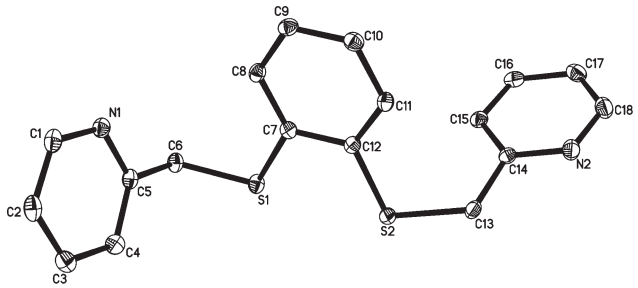

Fig. 2 Molecular structure of **L** with 30% probability level ellipsoids. Hydrogen atoms are omitted for clarity.

Table 1 Selected bond lengths (Å) and angles (°) for **L**

S(1)–C(7)	1.770(2)	C(7)–S(1)–C(6)	105.05(9)
S(1)–C(6)	1.813(2)	C(12)–S(2)–C(13)	103.64(10)
S(2)–C(12)	1.779(2)	C(5)–N(1)–C(1)	117.14(16)
S(2)–C(13)	1.804(2)	C(18)–N(2)–C(14)	117.27(19)
N(1)–C(1)	1.342(3)	C(5)–C(6)–S(1)	114.94(13)
N(1)–C(5)	1.335(2)	N(1)–C(5)–C(4)	122.74(18)
N(2)–C(14)	1.347(2)	C(14)–C(13)–S(2)	116.72(14)
N(2)–C(18)	1.339(3)	N(2)–C(14)–C(15)	122.59(17)

Synthesis and characterization of mononuclear Ni complexes Ni[1,2-(2-$C_5H_4NCH_2S)_2C_6H_4$]X_2 (1–3; X = Cl, Br, I) and Ni[1-(2-$C_5H_4NCH_2S$)-2-(2-$C_5H_4NCH_2SC_6H_4S$)C_6H_4]Br_2 (2*)

Similar to the previously reported $[N_2S_2]$-type ligand containing transition metal complexes,[23–25] the new mononuclear Ni complexes Ni[1,2-(2-$C_5H_4NCH_2S)_2C_6H_4$]X_2 (**1**, X = Cl; **2**, X = Br; **3**, X = I) could be prepared by reaction of the tetradentate $[N_2S_2]$-type ligand 1,2-(2-$C_5H_4NCH_2S)_2C_6H_4$ (**L**) with 1 equiv of $NiCl_2{\cdot}6H_2O$ in methanol or 1 equiv of anhydrous $NiBr_2$ or NiI_2 in ethyl alcohol at a given temperature in 82–88% yields. However, to our surprise, a novel mononuclear Ni complex **2*** was also obtained along with the expected complex **2** in 5% yield (Scheme 2). So far, although we do not know the detailed pathway for production of the unexpected complex **2***, it could be formally regarded as produced from insertion of the *in situ* generated fragment $[C_6H_4S]$ (possibly *via* cleavage of the corresponding C–S bonds in free ligand **L**) into the C–S bond of group SCH_2Py in ligand **L** of product **2** followed by the corresponding S → Ni coordination step.

Complexes **1–3** and **2*** are air-stable in the solid state and in solution, and were characterized by elemental analysis and various spectroscopies. For example, the IR spectra of **1–3** and **2*** each showed one absorption band in the range 1477–1433 cm^{-1} and one band in the range 752–743 cm^{-1} for

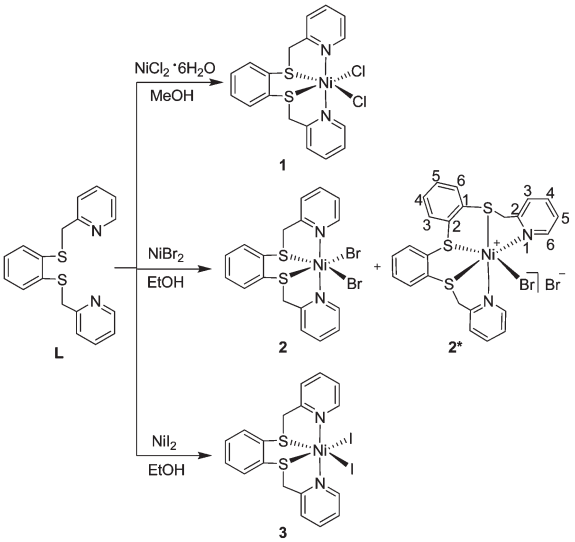

Scheme 2

their C═N double bonds and C–S single bonds, respectively. The ^{1}H NMR spectra of **1–3** and **2*** displayed a broad singlet at *ca.* 4.3 ppm for H atoms in their CH_2 groups and two broad singlets at *ca.* 7.7 and 8.5 ppm for 4-H and 6-H atoms in their pyridine rings, presumably due to their paramagnetic properties (see the ESI†). The ^{13}C NMR spectra of **2** and **3** each displayed one signal at *ca.* 38 ppm for C atoms in their CH_2 groups and five signals at *ca.* 122, 123, 137, 149, and 157 ppm assigned to 5-C, 3-C, 4-C, 6-C and 2-C atoms in their pyridine rings, respectively.

Synthesis and characterization of trinuclear $NiFe_2$ cluster complex Ni{[1,2-(2-$C_5H_4NCH_2S)_2C_6H_4$}$Fe_2(CO)_6(\mu_3$-S)$_2$ (4)

On the basis of synthesizing those new mononuclear Ni complexes **1–3**, we further prepared trinuclear $NiFe_2$ complex **4** by sequential reaction of $(\mu$-$S_2)Fe_2(CO)_6$ with 2 equiv of Et_3BHLi in THF at −78 °C, followed by treatment of the resulting intermediate $(\mu$-LiS$)_2Fe_2(CO)_6$ [26] with 1 equiv of mononuclear Ni complex **1**, **2** or **3** from −78 °C to room temperature in 12–20% yields, respectively (Scheme 3).

Interestingly, trinuclear complex **4** is the first butterfly $[Fe_2S_2]$ cluster complex with a tetradentate ligand **L**, although some similar trinuclear $NiFe_2$ complexes have been previously reported.[27–29] Trinuclear complex **4** is a deep-red and air-sensitive solid, which has been characterized by elemental analysis and HR-ESI-MS, IR, ^{1}H NMR, and ^{13}C NMR spectroscopies. For instance, the HR-ESI-MS showed an ion peak at m/z = 726.8012, corresponding to its protonated molecular ion $[M + H]^+$. The IR spectrum of **4** exhibited three absorption bands in the range 2049–1962 cm^{-1} for its terminal carbonyls and two bands at 1436 and 743 cm^{-1} for its C═N double bonds and C–S single bonds, respectively. The ^{1}H NMR spectrum of **4** displayed one broad singlet at 4.28 ppm for hydrogen atoms in its CH_2 groups, three broad singlets at 7.25, 7.71, and 8.47 ppm for 5-H, 4-H, and 6-H in its pyridine rings, probably also due to its paramagnetic property (see the ESI†). The ^{13}C NMR spectrum of **4** displayed one signal at 38.3 ppm for carbon atoms in its CH_2 groups and five signals at 122.4, 123.2, 136.9, 149.0, and 157.0 ppm for its 5-C, 3-C, 4-C, 6-C and 2-C atoms in its pyridine rings, respectively. In addition, the ^{13}C NMR spectrum of **4** also showed one signal at 212.5 ppm for its terminal carbonyls.

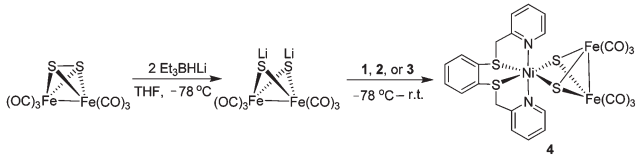

Scheme 3

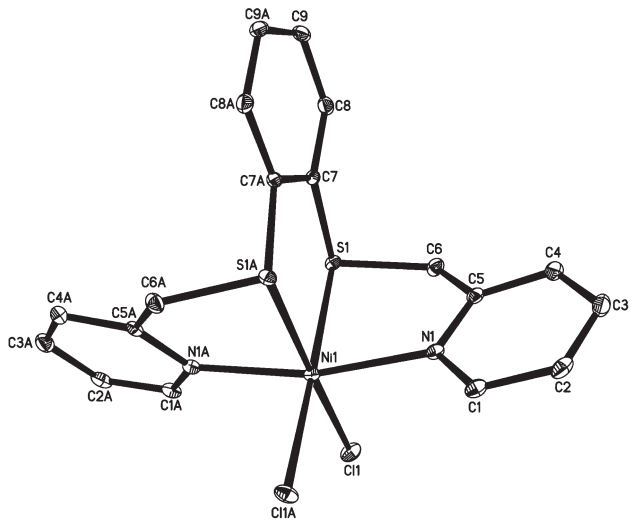

Fig. 3 Molecular structure of **1** with 30% probability level ellipsoids. Hydrogen atoms are omitted for clarity.

Crystal structures of mononuclear Ni complexes 1, 2*, and 3

Although we did not obtain the crystal structure of trinuclear complex **4** due to the lack of a suitable single crystal for X-ray diffraction analysis, we have successfully determined the crystal structures of its precursors **1** and **3**, as well as the unexpected mononuclear complex **2***. It is apparent that these crystal structures have not only further confirmed their own structures, but also provided the important structural information for trinuclear complex **4**. The ORTEP plots of **1**, **3**, and **2*** are shown in Fig. 3–5, and Table 2 lists their selected bond lengths and angles. Since **1** and **3** are actually isostructural, we mainly discuss some details about the crystal structure of **1**. As can be seen in Fig. 3, complex **1** contains one tetradentate ligand **L** and two monodentate chloro ligands which are attached to Ni(1) through S(1), S(1A), N(1), N(1A), Cl(1) and Cl(1A) atoms. The metal Ni(1) atom actually adopts a distorted octahedral geometry with the bond angles of ∠Cl(1)–Ni(1)–Cl(1A) = 94.01° and ∠N(1)–Ni(1)–N(1A) = 166.58°. The two bond angles of complex **1** are very close to the corresponding ones reported for *cis*-$[NiCl_2(C_{14}H_{16}N_2S_2)]$ (96.00° and 167.79°),[25] *cis*-$[NiCl_2(C_{15}H_{18}N_2S_2)]$ (94.88° and 166.48°)[30a] and *cis*-$[NiCl_2(C_{14}H_{14}S_3N_2S_2)]$

(100.59° and 164.32°).[30b] The bond lengths of Ni(1)–N(1), Ni(1)–Cl(1), and Ni(1)–S(1) are 2.1237, 2.3735, and 2.3970 Å, respectively. These bond lengths of complex **1** are also very close to the corresponding bond lengths reported for *cis*-[$NiCl_2(C_{14}H_{16}N_2S_2)$] (Ni–N/2.1078, Ni–Cl/2.3855, and Ni–S/2.4316 Å),[25] *cis*-[$NiCl_2(C_{15}H_{18}N_2S_2)$] (Ni–N/2.104, Ni–Cl/2.392, and Ni–S/2.451 Å),[30a] and *cis*-[$NiCl_2(C_{14}H_{14}S_3N_2S_2)$] (Ni–N/2.103, Ni–Cl/2.3435, and Ni–S/2.4763 Å).[30b] The bond lengths of Ni(1)–N(1) (2.115 Å) and Ni(1)–S(1) (2.3777 Å) in complex **3** are even shorter than those in complex **1**. Since the dihedral angle between the two planes involving S(1)/Ni(1)/S(1A) atoms and Cl(1)/Ni(1)/Cl(1A) atoms is only 0.4°, the five atoms S(1), S(1A), Cl(1), Cl(1A), and Ni(1) are virtually coplanar. This molecule has the two-fold crystallographic symmetry with a *cis*-S_2/*cis*-Cl_2/*trans*-N_2 geometrical configuration. It follows that the crystal structure of **1** is very similar to that of [N_2S_2]-type ligand-containing complexes such as *cis*-[$NiCl_2(C_{14}H_{16}N_2S_2)$],[25] *cis*-[$NiCl_2(C_{15}H_{18}N_2S_2)$],[30a] and *cis*-[$NiCl_2(C_{14}H_{14}S_3N_2S_2)$].[30b]

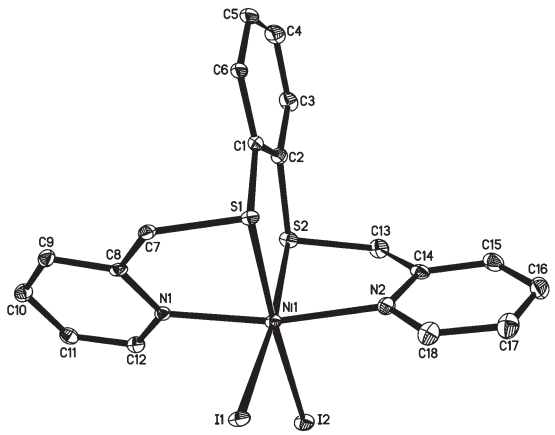

Fig. 4 Molecular structure of **3** with 30% probability level ellipsoids. Hydrogen atoms are omitted for clarity.

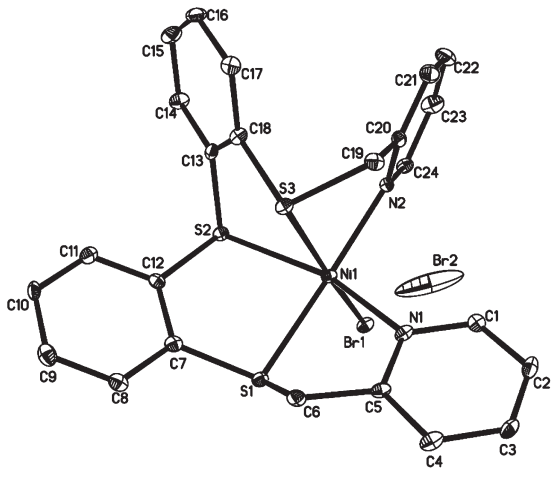

Fig. 5 Molecular structure of **2*** with 30% probability level ellipsoids. Hydrogen atoms are omitted for clarity.

Fig. 5 shows that complex **2*** consists of a pentadentate ligand 1-(2-$C_5H_4NCH_2S$)-2-(2-$C_5H_4NCH_2SC_6H_4S$)C_6H_4 and one monodentate bromo ligand, which are bound to Ni(1) *via* S(1), S(2), S(3), N(1) and N(2) atoms, respectively. Although the coordination geometry of the metal Ni(1) atom in **2*** is also a distorted octahedron, the structure of **2*** is considerably different to that of **1**, **3** and the above-mentioned *cis*-[$NiCl_2(C_{14}H_{16}N_2S_2)$][25] and *cis*-[$NiCl_2(C_{15}H_{18}N_2S_2)$][30a] by having a *cis*-S(1)-S(2)/*trans*-S(3)Br(1)/*cis*-N(1)N(2) geometric configuration. Another striking difference between their structures is that in **2*** one of the two halogen atoms is as anion Br^- located in the outside of the coordination sphere of central Ni(1) atom. Thus, while complex **1**, **3**, *cis*-[$NiCl_2(C_{14}H_{16}N_2S_2)$],[25] and *cis*-[$NiCl_2(C_{15}H_{18}N_2S_2)$],[30a] and *cis*-[$NiCl_2(C_{14}H_{14}S_3N_2S_2)$][30b] are neutral complexes each with a neutral Ni atom, **2*** is a cationic complex with a positively charged Ni atom. In addition, the dihedral angle between the two planes involving S(1)/Ni(1)/S(2) atoms and N(1)/Ni(1)/N(2) atoms is 10.7°, which is much larger than the corresponding one for **1**, and thus the five atoms S(1), S(2), Ni(1), N(1) and N(2) are not coplanar. It is worth pointing out that such cationic Ni complexes with a $[NiS_3N_2Br]^+$ core (which are actually similar to **2***) were previously reported by Drew.[31] The Ni(1)–Br(1) distance (2.5132 Å) of **2*** is slightly shorter than that (2.578 Å) in the corresponding cationic complex reported by Drew. Particularly notable is that complex

Table 2 Selected bond lengths (Å) and angles (°) for **1**, **3**, and **2***

1		**3**		**2***	
Ni(1)–N(1)	2.1237(18)	Ni(1)–N(1)	2.115(3)	Ni(1)–N(1)	2.088(5)
Ni(1)–N(1A)	2.1236(18)	Ni(1)–N(2)	2.112(3)	Ni(1)–N(2)	2.100(5)
Ni(1)–Cl(1)	2.3735(8)	Ni(1)–I(1)	2.7685(5)	Ni(1)–Br(1)	2.5132(14)
Ni(1)–Cl(1A)	2.3735(8)	Ni(1)–I(2)	2.7452(5)	N(2)–C(24)	1.346(9)
Ni(1)–S(1)	2.3970(8)	Ni(1)–S(1)	2.3777(9)	Ni(1)–S(1)	2.389(2)
Ni(1)–S(1A)	2.3969(8)	Ni(1)–S(2)	2.3811(9)	Ni(1)–S(2)	2.474(2)
N(1)–C(1)	1.343(3)	N(1)–C(12)	1.343(4)	N(1)–C(1)	1.351(8)
S(1)–C(6)	1.806(2)	N(2)–C(14)	1.344(4)	N(1)–C(5)	1.356(8)
N(1)–Ni(1)–N(1A)	166.58(9)	N(1)–Ni(1)–N(2)	168.07(11)	N(1)–Ni(1)–N(2)	98.0(2)
N(1)–Ni(1)–Cl(1)	92.29(5)	N(1)–Ni(1)–I(1)	88.61(7)	N(1)–Ni(1)–S(1)	80.95(16)
N(1A)–Ni(1)–Cl(1)	96.86(5)	N(1)–Ni(1)–I(2)	98.93(8)	N(2)–Ni(1)–S(1)	175.64(16)
N(1A)–Ni(1)–Cl(1A)	92.29(5)	N(1)–Ni(1)–S(1)	83.47(8)	N(1)–Ni(1)–Br(1)	95.39(15)
Cl(1)–Ni(1)–Cl(1A)	94.01(4)	N(1)–Ni(1)–S(2)	87.23(8)	N(2)–Ni(1)–Br(1)	94.56(15)
Cl(1)–Ni(1)–S(1A)	176.67(2)	I(1)–Ni(1)–S(1)	85.90(2)	S(1)–Ni(1)–S(2)	82.90(6)
Cl(1A)–Ni(1)–S(1A)	89.30(3)	I(1)–Ni(1)–S(2)	172.60(3)	S(1)–Ni(1)–Br(1)	89.77(6)
Cl(1)–Ni(1)–S(1)	89.30(3)	S(1)–Ni(1)–S(2)	87.54(3)	S(2)–Ni(1)–S(3)	80.93(6)

2* is the first crystallographically characterized mononuclear Ni complex with an unusual ligand of 1-(2-$C_5H_4CH_2S$)-2-(2-$C_5H_4NCH_2SC_6H_4S$)C_6H_4.

Electrochemical study of 1–4

The electrochemical properties of the mononuclear and trinuclear complexes of **1–3** and **4** were studied by using cyclic voltammetry. Table 3 lists their electrochemical data, and Fig. 6 and 7 present their cyclic voltammograms. As shown in Table 3 and Fig. 6, the mononuclear complexes **1–3** each display two irreversible reduction processes in the range from −1.18 to −1.80 V and their two reduction potentials are decreased respectively in the order of **1** to **2** and then to **3**. That is, the reductions of **1–3** become easier from chloride to bromide to iodide, which is consistent with the case previously reported by Darensbourg and co-workers.[32] All the two reduction processes of **1–3** are one-electron processes, which are supported by the calculated value of 1.09 faraday/equiv (obtained by study of bulk electrolysis of **3** at −1.23 V) and could be assigned to reductions of Ni^{II} to Ni^{I} and Ni^{I} to Ni^{0}, respectively.[33] Complexes **1–3** also show three irreversible oxidation processes in the region from −0.35 to +1.30 V. The first sharp oxidation peaks at −0.40 V for **1**/**2** and at −0.35 V for **3** could be ascribed to the oxidation processes of the corresponding reduced products of **1–3**. This is because all the first three oxidation peaks for **1–3** did not appear during the positive direction scanning course starting from −1 V. In addition, similar cases for such assignments regarding the first three oxidation peaks of **1–3** were also found in the literature.[34] In order to assign another two oxidation processes of **1–3**, we determined the cyclic voltammograms of *n*-Bu_4NX (X = Cl, Br, I) under similar conditions for comparison. As a result, the voltammograms of *n*-Bu_4NX showed one quasi-reversible oxidation peak at +0.64 V for *n*-Bu_4NCl, one at +0.28 V for *n*-Bu_4NBr, and one at −0.01 V for *n*-Bu_4NI, respectively. Through comparison of oxidation potentials of the three halides with the corresponding those of **1–3**, we could conclude that the three oxidation peaks at +0.86 V for **1**, at +0.32 V for **2**, and at −0.12 V for **3** might be attributed to oxidations of the corresponding halide ligands in **1–3**. The third irreversible oxidation peak at +1.30 V for **1**, at +0.67 V for **2**, and at +0.28 V for **3** is most likely generated from the oxidation processes from Ni^{II} to Ni^{III} in the three mononuclear complexes. It is noteworthy that these oxidation potentials for the oxidations from Ni^{II} to Ni^{III} in **1–3** are much higher than those (usually in the range from −0.08 to +0.57 V *vs.* Fc/Fc^{+}) reported for some Ni^{II}-containing complexes.[24,35–38] This means that the oxidation potentials from Ni^{II} to Ni^{III} in such Ni^{II} complexes are very sensitive to the structure and composition of the Ni^{II}-containing complexes. Interestingly, as shown in Table 3 and Fig. 7, trinuclear complex **4** displays four irreversible reduction processes at −1.05, −1.31, −1.52 and −1.97. Through comparison of these reduction potentials with those of some reported [NiFe]-hydrogenase model complexes containing the [NS]-type ligands (usually their reduction potentials of Ni^{II} are in the range −0.8 to −1.2 V)[32,33,39–41] and some reported similar [FeFe]-hydrogenase model complexes (usually their first reduction potentials from $Fe^{I}Fe^{I}$ to $Fe^{I}Fe^{0}$ are in the range −1.4 to −1.8 V *vs.* Fc/Fc^{+}),[33,42–44]

Table 3 Electrochemical data of **1–4**[a]

Complex	E_{pc} (V)	E_{pa} (V)
1	−1.55	−0.40[b]
	−1.80	+0.86
		+1.30
2	−1.31	−0.40[b]
	−1.55	+0.32
		+0.67
3	−1.18	−0.35[b]
	−1.51	−0.12
		+0.28
4	−1.05	−0.55[b]
	−1.31	−0.24
	−1.52	+0.88
	−1.97	

[a] All potentials *versus* Fc/Fc^{+}. [b] Oxidation potentials of the reduced products.

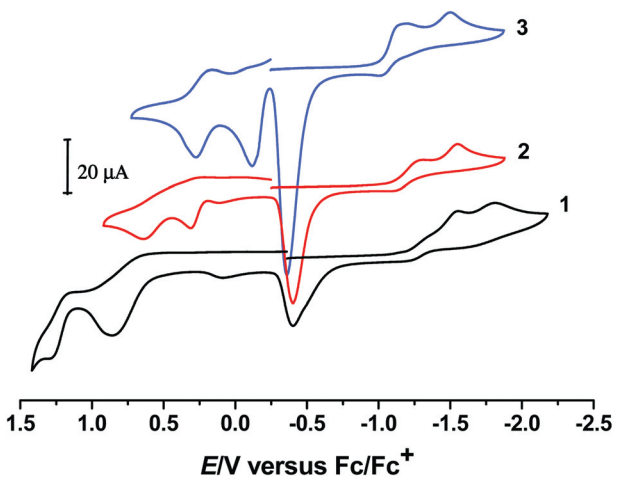

Fig. 6 Cyclic voltammogram of **1** (1.0 mM), **2** (0.6 mM) and **3** (1.0 mM) in 0.1 M *n*-Bu_4NPF_6/MeCN at a scan rate of 100 mV s^{-1}.

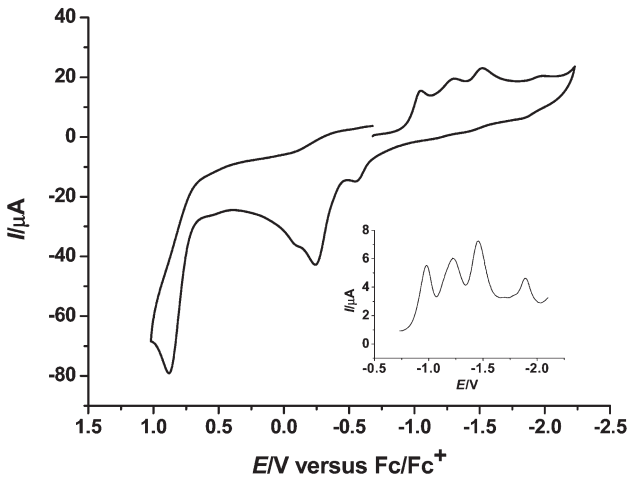

Fig. 7 Cyclic voltammogram of **4** (1.0 mM) in 0.1 M *n*-Bu_4NPF_6/MeCN at a scan rate of 100 mV s^{-1}.

the former two peaks at −1.05 and −1.31 V should be attributed to the one-electron reduction processes of **4** involving $Ni^{II} \rightarrow Ni^{I}$ and $Ni^{I} \rightarrow Ni^{0}$, while the latter two peaks at −1.52 and −1.97 V could be ascribed to $Fe^{I}Fe^{I} \rightarrow Fe^{I}Fe^{0}$ and $Fe^{I}Fe^{0} \rightarrow Fe^{0}Fe^{0}$, respectively. The oxidation peak at −0.24 V for **4** might be assigned to $Ni^{II} \rightarrow Ni^{III}$ oxidation process, which is shifted toward the negative direction by 1140 mV relative to the corresponding potential +0.90 V (*vs.* Fc/Fc^{+}) of the cationic $[Ni(DtdtzH_2)]^{2+}$ complex[34] and toward the positive direction shifted by 190 mV relative to the corresponding potential −0.43 V (*vs.* Fc/Fc^{+}) of the anionic $[Ni(pdtc)_2]^{2-}$ complex[45] and very close to the corresponding oxidation potential −0.11 V (*vs.* Fc/Fc^{+}) of the neutral complex Ni(dtdtz).[34] Since the irreversible oxidation peak of **4** at +0.88 V displays two-fold peak current of the reduction peak at −1.52 V, it should be assigned as a two-electron oxidation process from the $Fe^{I}Fe^{I}$ to $Fe^{II}Fe^{II}$couple.[46,47]

The cyclic voltammogram of **4** in the presence of HOAc and without HOAc (for comparison) is shown in Fig. 8. As shown in Fig. 8, when the first 2 mM HOAc were added, the first three reduction peaks of **4** slightly increased, but they did not grow with sequential addition of the acid from 2 to 10 mM. However, upon addition of 2–10 mM HOAc, the original reduction peak at −1.97 V was slightly shifted to more negative potentials and grew remarkably with increasing concentration of HOAc. Such rapid increases in current heights of these reduction peaks are characteristic of an electrocatalytic process for proton reduction to hydrogen. Interestingly, this catalytic process was further confirmed by bulk electrolysis of a MeCN solution of **4** (0.5 mM) with excess HOAc (Fig. 9). The initial rate of electrolysis is more than 3 times than that in the absence of catalyst **4**. A total of 12.4 F per mol of **4** passed in 0.5 h with 6.2 turnovers. Gas chromatographic analysis indicated that the bulk electrolysis produced H_2 in 70% yield. It should be noted that this is the first example for the electrocatalytic H_2 evolution from the weak acid HOAc catalyzed by a [NiFe]-hydrogenase model complex, although some examples for the CF_3CO_2H proton reduction to give H_2 catalyzed by some [NiFe]-hydrogenase model complexes were previously reported.[48–50]

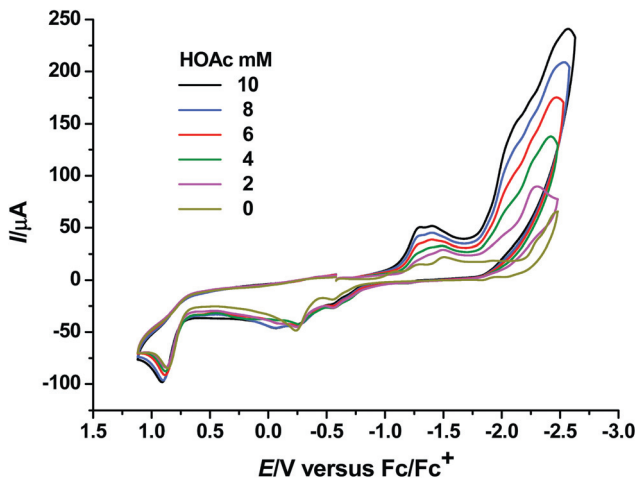

Fig. 8 Cyclic voltammograms of **4** (1.0 mM) with HOAc (0–10 mM) in 0.1 M *n*-Bu_4NPF_6/MeCN at a scan rate of 100 mV s^{-1}.

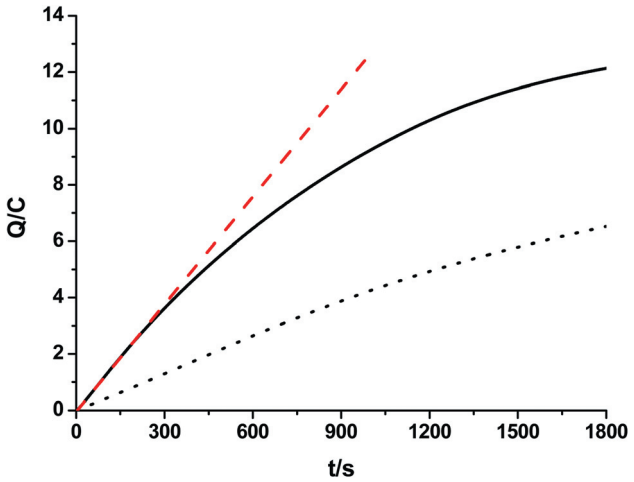

Fig. 9 Bulk electrolysis of HOAc (12.5 mM) at a vitreous carbon rod electrode in the presence of **4** (—) and absence of **4** (···); extrapolation of the catalytic reduction at the initial electrolysis rate (---).

Conclusions

The $[N_2S_2]$-type ligand **L** was prepared by a new method and its structure confirmed by X-ray crystal diffraction analysis. The new mononuclear Ni complexes **1–3** and **2*** have been synthesized by reaction of ligand **L** with $NiCl_2{\cdot}6H_2O$, $NiBr_2$, or NiI_2 under mild conditions. Interestingly, while **1–3** are the expected neutral complexes, cationic complex **2*** is produced unexpectedly along with **2**. More interestingly, the reaction of mononuclear Ni complexes **1**, **2**, or **3** with the *in situ* formed $(\mu\text{-LiS})_2Fe_2(CO)_6$ results in formation of the novel trinuclear $NiFe_2$ complex **4**, a structural analogue of the active site of [NiFe]Hases. All the new complexes **1–4** and **2*** are fully characterized by elemental analysis and various spectroscopic techniques. The molecular structures of **1**, **3**, and **2*** are unambiguously confirmed by X-ray crystallography, and some electrochemical properties of **1–4** have been studied by cyclic voltammetry. Further investigations on application of mononuclear Ni complexes **1–3** to prepare other Ni–Fe complexes as model compounds for the active site of [NiFe]Hases are in progress in this laboratory.

Experimental section

General comments

All reactions involving air-sensitive compounds were carried out using standard Schlenk or vacuum-line techniques under an atmosphere of prepurified nitrogen. Tetrahydrofuran (THF) was dried and deoxygenated by distillation from sodium–benzophenone ketyl. Et_3BHLi (1 M in THF), 2-(chloromethyl)pyridine hydrochloride, $NiCl_2{\cdot}6H_2O$, anhydrous NiX_2 (X = Br, I) and other chemicals were available commercially and used as received. $(\mu\text{-}S_2)Fe_2(CO)_6$[51] and 1,2-benzenedithiol[52] were prepared according to the literature procedures. Preparative thin-layer chromatography (TLC) was carried out on fluorescent glass plates (26 × 20 × 0.25 cm) coated with silica gel GF 254 (10–40 μm). IR spectra were recorded on a Bio-Rad FTS 6000

spectrophotometer. ^{1}H NMR and ^{13}C NMR spectra were taken on a Bruker Avance 300 or 400 NMR spectrometer. Analysis and assignments of the ^{1}H and ^{13}C NMR spectroscopic data were supported by ^{1}H-^{1}H COSY, ^{1}H-^{1}H NOESY, ^{1}H-^{13}C HMQC (heteronuclear multiple quantum coherence), and ^{1}H-^{13}C HMBC (heteronuclear multiple bond correlation) experiments. ESI-MS determinations were performed by using LCQ Advantage LC/MS spectrometers. Elemental analyses were performed on an Elementar Vario EL analyzer. Melting points were determined on a Yanaco Mp-500 apparatus and were uncorrected.

Preparation of 1,2-(2-$C_5H_4NCH_2S)_2C_6H_4$ (L)

In a 100 mL two-necked flask fitted with a magnetic stir-bar, a rubber septum and a nitrogen inlet tube was dissolved metallic sodium (0.920 g, 40.0 mmol) in absolute ethanol (20 mL) and then a solution of 1,2-benzenedithiol (1.420 g, 10.0 mmol) in absolute ethanol (5 mL) was added. After the mixture was stirred at room temperature for 15 min, a solution of 2-(chloromethyl) pyridine hydrochloride (3.280 g, 20.0 mmol) in absolute ethanol (5 mL) was added. The new mixture was stirred for additional 0.5 h and then it was heated to reflux and stirred at this temperature for 6 h. Once cooled to room temperature, the white precipitates were filtered out from the orange-red solution and then washed with CH_2Cl_2 (3 × 15 mL). After the washings were combined with the separated orange-red solution, volatiles were removed at reduced pressure and the residue was subjected to TLC separation using petroleum ether–ethyl acetate (1 : 1 v/v) as eluent. The eluate derived from the main orange band was evaporated under vacuum to give initially an orange oil and then it solidified as a yellowish solid (2.715 g, 84%), mp 60–62 °C. Anal. Calcd for $C_{18}H_{16}N_2S_2$: C, 66.63; H, 4.79; N, 8.63. Found: C, 66.60; H, 5.03; N, 8.61. IR (KBr disk): $\nu_{C=N}$ 1641 (m); ν_{C-S} 746 (m) cm^{-1}. ^{1}H NMR (400 MHz, $CDCl_3$, TMS): 4.27 (s, 4H, PyC*H*$_2$), 7.04–7.06 (m, 2H, 4,5-Ph*H*), 7.12–7.15 (m, 2H, 5-Py*H*), 7.23–7.25 (m, 2H, 3,6-Ph*H*), 7.29 (d, 2H, *J* = 8.0 Hz, 3-Py*H*), 7.57 (td, 2H, *J* = 8.0 and 2.0 Hz, 4-Py*H*), 8.53 (d, 2H, *J* = 4.0 Hz, 6-Py*H*) ppm. ^{13}C NMR (100 MHz, $CDCl_3$, TMS): 39.8 (Py*C*H$_2$), 122.1 (5-Py*C*H), 123.2 (3-Py*C*H), 126.9 (4,5-Ph*C*H), 130.0 (3,6-Ph*C*H), 136.5 (1,2-Ph*C*), 136.6 (4-Py*C*H), 149.3 (6-Py*C*H), 157.4 (2-Py*C*) ppm. ^{1}H NMR (400 MHz, DMSO-d_6, TMS): 4.30 (s, 4H, PyC*H*$_2$), 7.10–7.13 (m, 2H, 4,5-Ph*H*), 7.24–7.27 (m, 2H, 5-Py*H*), 7.34–7.36 (m, 2H, 3,6-Ph*H*), 7.38 (d, 2H, *J* = 8.0 Hz, 3-Py*H*), 7.72 (td, 2H, *J* = 8.0 and 2.0 Hz, 4-Py*H*), 8.48 (d, 2H, *J* = 4.4 Hz, 6-Py*H*) ppm. ^{13}C NMR (100 MHz, DMSO-d_6, TMS): 38.5 (Py*C*H$_2$), 122.3 (5-Py*C*H), 123.1 (3-Py*C*H), 126.3 (4,5-Ph*C*H), 128.5 (3,6-Ph*C*H), 135.6 (1,2-Ph*C*), 136.8 (4-Py*C*H), 149.0 (6-Py*C*H), 157.1 (2-Py*C*) ppm. ESI-MS (CH_2Cl_2): *m*/*z* = 325 (M^+ + H).

Preparation of Ni[1,2-(2-$C_5H_4NCH_2S)_2C_6H_4$]Cl_2 (1)

A greenish solution of $NiCl_2{\cdot}6H_2O$ (1.691 g, 7.1 mmol) in methanol (15 mL) was slowly added to a stirred solution of **L** (2.302 g, 7.1 mmol) in methanol (15 mL) at room temperature. During the course of addition, some blue precipitates were produced. The mixture continued to be stirred at room temperature for 1 h and then the blue precipitates were collected by filtration, washed successively with methanol (3 × 5 mL) and diethyl ether (3 × 5 mL), and finally dried *in vacuo*. **1** was obtained as a blue solid (2.820 g, 88%), mp >250 °C. Anal. Calcd for $C_{18}H_{16}Cl_2N_2NiS_2$: C, 47.61; H, 3.55; N, 6.17. Found: C, 47.51; H, 3.58; N, 6.17. IR (KBr disk): $\nu_{C=N}$ 1473 (s); ν_{C-S} 752 (s) cm^{-1}. ^{1}H NMR (400 MHz, DMSO-d_6, TMS): 4.32 (br.s, 4H, PyC*H*$_2$), 7.11 (br.s, 2H, 4,5-Ph*H*), 7.34 (br.s, 6H, 3,5-Py*H*, 3,6-Ph*H*), 7.74 (br.s, 2H, 4-Py*H*), 8.52 (br.s, 2H, 6-Py*H*) ppm. ^{13}C NMR data of this compound could not be obtained due to its very low solubility in common solvents. ESI-MS (DMSO): *m*/*z* = 492 (M^+ + K).

Preparation of Ni[1,2-(2-$C_5H_4NCH_2S)_2C_6H_4$]Br_2 (2) and Ni[1-(2-$C_5H_4NCH_2S$)-2-(2-$C_5H_4NCH_2SC_6H_4S$)C_6H_4]Br_2 (2*)

A greenish suspension of anhydrous $NiBr_2$ (1.448 g, 6.5 mmol) in 95% ethanol (75 mL) was added to a stirred solution of **L** (2.104 g, 6.5 mmol) in ethanol (20 mL) at room temperature. The mixture was stirred at about 35 °C for 3 h and then was filtered to give some blue precipitates. After the blue precipitates were washed with ethanol (3 × 5 mL) and diethyl ether (3 × 5 mL), and finally dried *in vacuo*, **2** was obtained as a blue solid (2.926 g, 82%). **2*** was obtained as a blue needle-shaped crystal (0.212 g, 5%) from the filtrate by slow evaporation of its solvent at room temperature for several weeks. **2**: mp >250 °C. Anal. Calcd for $C_{18}H_{16}Br_2N_2NiS_2$: C, 39.82; H, 2.97; N, 5.16. Found: C, 39.87; H, 2.83; N, 5.17. IR (KBr disk): $\nu_{C=N}$ 1473 (s); ν_{C-S} 752 (s) cm^{-1}. ^{1}H NMR (400 MHz, DMSO-d_6, TMS): 4.30 (br.s, 4H, PyC*H*$_2$), 7.11 (br.s, 2H, 4,5-Ph*H*), 7.25 (br.s, 2H, 5-Py*H*), 7.34 (br.s, 2H, 3,6-Ph*H*), 7.37 (br.s, 2H, 3-Py*H*), 7.72 (br.s, 2H, 4-Py*H*), 8.48 (br.s, 2H, 6-Py*H*) ppm. ^{13}C NMR (100 MHz, DMSO-d_6, TMS): 38.6 (Py*C*H$_2$), 122.4 (5-Py*C*H), 123.2 (3-Py*C*H), 126.4 (4,5-Ph*C*H), 128.6 (3,6-Ph*C*H), 136.6 (1,2-Ph*C*), 136.8 (4-Py*C*H), 149.0 (6-Py*C*H), 157.0 (2-Py*C*) ppm. ESI-MS (DMSO): *m*/*z* = 541 (M^+ + H). **2***: mp 183–185 °C. Anal. Calcd for $C_{24}H_{20}Br_2N_2NiS_3$: C, 44.27; H, 3.10; N, 4.30. Found: C, 43.92; H, 3.41; N, 4.26. IR (KBr disk): $\nu_{C=N}$ 1444 (m); ν_{C-S} 747 (vs) cm^{-1}. ^{1}H NMR (400 MHz, DMSO-d_6, TMS): 4.32 (br.s, 4H, PyC*H*$_2$S), 6.93 (br.s, 2H, 3-Ph*H*), 7.12 (br.s, 2H, 4-Ph*H*), 7.24 (br.s, 4H, 5-Py*H*, 5-Ph*H*), 7.36 (br.s, 2H, 3-Py*H*), 7.43 (br.s, 2H, 6-Ph*H*), 7.68 (br.s, 2H, 4-Py*H*), 8.46 (br.s, 2H, 6-Py*H*) ppm. ^{13}C NMR (100 MHz, DMSO-d_6, TMS): 38.2 (Py*C*H$_2$S), 122.3 (5-Py*C*H), 123.1 (3-Py*C*H), 126.7 (4-Ph*C*H), 127.9 (5-Ph*C*H), 128.6 (6-Ph*C*H), 130.9 (3-Ph*C*H), 133.1 (2-Ph*C*), 136.5 (4-Py*C*H), 137.8 (1-Ph*C*), 148.8 (6-Py*C*H), 156.7 (2-Py*C*) ppm. ESI-MS (DMSO): *m*/*z* = 569 $(M - Br)^+$.

Preparation of Ni[1,2-(2-$C_5H_4NCH_2S)_2C_6H_4$]I_2 (3)

A greenish suspension of anhydrous NiI_2 (1.969 g, 6.3 mmol) in 95% ethanol (50 mL) was added to a stirred solution of **L** (2.027 g, 6.3 mmol) in ethanol (20 mL) at room temperature to give a mixture with some green precipitates. The mixture was heated to reflux for 2 h and then the green precipitates were collected by filtration, washed with ethanol (3 × 5 mL) and diethyl ether (3 × 5 mL), and finally dried *in vacuo*. **3** was obtained as a green solid (3.475 g, 87%), mp >230 °C. Anal. Calcd for

$C_{18}H_{16}I_2N_2NiS_2$: C, 33.94; H, 2.53; N, 4.40. Found: C, 34.03; H, 2.65; N, 4.30. IR (KBr disk): $\nu_{C\equiv N}$ 1477 (s); ν_{C-S} 751 (s) cm^{-1}. ^1H NMR (400 MHz, DMSO-d_6, TMS): 4.29 (br.s, 4H, PyCH_2), 7.10 (br.s, 2H, 4,5-Ph*H*), 7.25 (br.s, 2H, 5-Py*H*), 7.35 (br.s, 4H, 3-Py*H*, 3,6-Ph*H*), 7.71 (br.s, 2H, 4-Py*H*), 8.47 (br.s, 2H, 6-Py*H*) ppm. ^{13}C NMR (100 MHz, DMSO-d_6, TMS): 38.4 (Py*C*H_2), 122.2 (5-Py*C*H), 123.1 (3-Py*C*H), 126.3 (4,5-Ph*C*H), 128.5 (3,6-Ph*C*H), 135.5 (1,2-Ph*C*), 136.7 (4-Py*C*H), 148.9 (6-Py*C*H), 156.9 (2-Py*C*) ppm. ESI-MS (DMSO): m/z = 509 ($M^+ - I$).

Preparation of [Ni{1,2-(2-$C_5H_4NCH_2S)_2C_6H_4$}]$Fe_2(CO)_6(\mu_3$-S)$_2$ (4)

A 100 mL two-necked flask equipped with a magnetic stir-bar, a serum cap, and a nitrogen inlet tube was charged with (μ-S)$_2$Fe$_2$(CO)$_6$ (0.086 g, 0.25 mmol) and THF (10 mL), which was stirred and cooled to −78 °C to give a red solution. To this solution was added Et_3BHLi (0.5 mL, 0.5 mmol) to give a (μ-LiS)$_2$Fe$_2$(CO)$_6$-containing green solution. After stirring this green solution at −78 °C for 15 min, **1** (0.114 g, 0.25 mmol), **2** (0.136 g, 0.25 mmol) or **3** (0.159 g, 0.25 mmol) was added. The new mixture was stirred at −78 °C for 2 h and at room temperature overnight to give a deep red solution. Volatiles were removed under vacuum, and the residue was subjected to column chromatography under anaerobic conditions. Elution with ethyl acetate afforded a main red band from which product **4** (0.022 g, 10%) derived from **1**, or product **4** (0.03 g, 14%) derived from **2**, or product **4** (0.043 g, 20%) derived from **3** was respectively obtained as a dark red solid. mp 63–65 °C. Anal. Calcd for $C_{24}H_{16}Fe_2N_2NiO_6S_4$: C, 39.65; H, 2.22; N, 3.85. Found: C, 39.71; H, 2.43; N, 3.82. IR (KBr disk): $\nu_{C\equiv O}$ 2049 (s), 2004 (vs), 1962 (vs); $\nu_{C\equiv N}$ 1436 (m); ν_{C-S} 743 (s) cm^{-1}. ^1H NMR (400 MHz, DMSO-d_6, TMS): 4.28 (br.s, 4H, PyCH_2), 7.11 (br.s, 2H, 4,5-Ph*H*), 7.25 (br.s, 2H, 5-Py*H*), 7.33 (br.s, 2H, 3,6-Ph*H*), 7.37 (d, 2H, J = 7.2 Hz, 3-Py*H*), 7.71 (br.s, 2H, 4-Py*H*), 8.47 (br.s, 2H, 6-Py*H*) ppm. ^{13}C NMR (100 MHz, DMSO-d_6, TMS): 38.3 (Py*C*H_2), 122.4 (5-Py*C*H), 123.2 (3-Py*C*H), 126.4 (4,5-Ph*C*H), 128.5 (3,6-Ph*C*H), 135.5 (1,2-Ph*C*), 136.9 (4-Py*C*H), 149.0 (6-Py*C*H), 157.0 (2-Py*C*), 212.5 (Fe*C*O) ppm. ESI-MS (DMSO): m/z = 727 (M^+ + H).

X-ray structure determinations of L, 1, 3 and 2*

The single crystals suitable for X-ray diffraction analyses were grown by the slow diffusion of hexane into a CH_2Cl_2 solution of **L** at room temperature or by slow evaporation MeOH–*n*-hexane solution of **1**, MeCN solution of **3** or EtOH solution of **2*** at room temperature, respectively. Each crystal was mounted on a Rigaku MM-007 (rotating anode) diffractometer equipped with Saturn 70CCD. Data were collected at room temperature, using a confocal monochromator with Mo-K_α radiation (λ = 0.71073 Å) in the ω–ϕ scanning mode. Data collection, reduction and absorption correction were performed using the CrystalClear program.[53] The structures were solved by direct methods using the SHELXS-97 program[54] and refined by full-matrix least-squares techniques (SHELXL-97)[55] on F^2. Hydrogen atoms were located by using the geometric method. Details of crystal data, data collections and structure refinements are summarized in Table 4.

Electrochemistry

Acetonitrile (DikmaPure Chemicals) used for the electrochemistry was HPLC grade. A solution of 0.1 M *n*-Bu_4NPF_6 in MeCN was used as the electrolyte in all CV experiments. The electrolyte solution was degassed by bubbling with N_2 for at least 10 min before measurement. Electrochemical measurements were performed on a BAS Epsilon potentiostat. All

Table 4 Crystal data and structure refinements details for **L**, **1**, **3**, and **2***

Compound	**L**	**1**	**3**	**2***
Formula	$C_{18}H_{16}N_2S_2$	$C_{18}H_{16}Cl_2N_2NiS_2{\cdot}2.5CH_3OH{\cdot}0.5C_6H_{14}$	$C_{18}H_{16}I_2N_2NiS_2$	$C_{24}H_{20}Br_2N_2NiS_3{\cdot}1.75H_2O{\cdot}0.5C_2H_5OH$
M_w	324.45	577.25	636.96	701.69
T (K)	113(2)	113(2)	113(2)	113(2)
Cryst syst	Orthorhombic	Monoclinic	Monoclinic	Triclinic
Space group	*Pbca*	*C*2/*c*	*C*2/*c*	$P\bar{1}$
a (Å)	9.472(5)	13.449(3)	17.910(2)	8.950(4)
b (Å)	9.871(6)	22.132(9)	19.919(2)	9.773(4)
c (Å)	32.954(17)	8.0234(16)	14.2714(14)	16.464(7)
α (°)	90	90	90	104.53(2)
β (°)	90	99.12(3)	128.341(4)	97.18(4)
γ (°)	90	90	90	16.464(7)
V (Å^3)	3081(3)	2358.0(12)	3993.3(7)	1346.4(9)
Z	8	4	8	2
Crystal size (mm)	0.20 × 0.18 × 0.12	0.20 × 0.18 × 0.12	0.26 × 0.24 × 0.22	0.20 × 0.18 × 0.10
D_c (g cm^{-3})	1.399	1.626	2.119	1.731
μ/mm^{-1}	0.343	1.256	4.277	3.947
F(000)	1360	1208	2432	705
Reflns collected	22 563	9981	18 921	9866
Reflns unique	3667	2082	4740	4643
$\theta_{mix/max}$ (°)	2.47/27.88	3.16/25.02	1.77/27.89	2.23/25.02
Final R	0.0471	0.0347	0.0328	0.0537
Final Rw	0.1043	0.0777	0.0799	0.1536
GOF on F^2	1.080	1.109	1.210	1.140
$\Delta\rho_{max/min}$ (e Å^{-3})	0.376/−0.250	0.382/−0.621	1.488/−1.982	3.276/−4.650

voltammograms were obtained in a conventional three-electrode cell, using a 3 mm diameter glassy carbon working electrode, a platinum wire counter electrode, and a nonaqueous Ag/Ag^+(0.01 M $AgNO_3$/0.1 M n-Bu_4NPF_6 in MeCN) reference electrode under N_2. The working electrode was polished with 0.05 μm alumina paste and sonicated in water for 10 min prior to use. Bulk electrolysis was run on a vitreous carbon rod (*ca.* 3 cm^2) in a two-compartment, gas tight, H-type electrolysis cell containing *ca.* 20 mL of MeCN. All potentials are referred to the ferrocene/ferrocenium (Fc/Fc^+). Gas chromatography was performed with a Shimadzu gas chromatograph GC-9A under isothermal conditions with nitrogen as a carrier gas and a thermal conductivity detector.

Acknowledgements

We are grateful to the National Natural Science Foundation of China (21132001, 20972073), 973 (2011CB935902) and the Tianjin Natural Science Foundation (09JCZDJC27900) for financial support.

References

1 R. Cammack, *Nature*, 1999, **397**, 214–215.
2 M. W. W. Adams and E. I. Stiefel, *Science*, 1998, **282**, 1842–1843.
3 R. K. Thauer, A. R. Klein and G. C. Hartmann, *Chem. Rev.*, 1996, **96**, 3031–3042.
4 P. M. Vignais and B. Billoud, *Chem. Rev.*, 2007, **107**, 4206–4272.
5 Y. Nicolet, B. J. Lemon, J. C. Fontecilla-Camps and J. W. Peters, *Trends Biochem. Sci.*, 2000, **25**, 138–143.
6 D. J. Evans and C. J. Pickett, *Chem. Soc. Rev.*, 2003, **32**, 268–275.
7 M. Frey, *ChemBioChem*, 2002, **3**, 153–160.
8 S. P. J. Albracht, *Biochim. Biophys. Acta, Bioenerg.*, 1994, **1188**, 167–204.
9 W. Luibtz, E. J. Reijerse and M. van Gastel, *Chem. Rev.*, 2007, **107**, 4331–4365.
10 (*a*) J. C. Fontecilla-Camps, A. Volbeda, C. Cavazza and Y. Nicolet, *Chem. Rev.*, 2007, **107**, 4273–4303; (*b*) R. Bouwman, *Coord. Chem. Rev.*, 2005, **249**, 1555–1581.
11 S. Shima, O. Pilak, S. Vogt, M. Schick, M. S. Stagni, W. Meyer-Klaucke, E. Warkentin, R. K. Thauer and U. Ermler, *Science*, 2008, **321**, 572–575.
12 S. Shima and R. K. Thauer, *Chem. Rec.*, 2007, **7**, 37–46.
13 J. A. Wright, P. J. Turrell and C. J. Pickett, *Organometallics*, 2010, **29**, 6146–6156.
14 (*a*) A. Volbeda, M.-H. Charon, C. Piras, E. C. Hatchikian, M. Frey and J. C. Fontecilla-Camps, *Nature*, 1995, **373**, 580–587; (*b*) A. Volbeda, E. Garcin, C. Piras, A. L. de Lacey, V. M. Fernandez, E. C. Hatchikian, M. Frey and J. C. Fontecilla-Camps, *J. Am. Chem. Soc.*, 1996, **118**, 12989–12996.
15 (*a*) Y. Higuchi, T. Yagi and N. Yasuoka, *Structure*, 1997, **5**, 1671–1680; (*b*) Y. Higuchi, H. Ogata, K. Miki, N. Yasuoka and T. Yagi, *Structure*, 1999, **7**, 549–556.
16 E. Carcin, X. Vernede, E. C. Hatchikian, A. Volbeda, M. Frey and J. C. Fontecilla-Camps, *Structure*, 1999, **7**, 557–566.
17 R. P. Happe, W. Roseboom, A. J. Pierik, S. P. J. Albracht and K. A. Bagley, *Nature*, 1997, **385**, 126–126.
18 J. C. Fontecilla-Camps, M. Frey, E. Garcin, C. Hatchikian, Y. Montet, C. Piras, X. Vernède and A. Volbeda, *Biochimie*, 1997, **79**, 661–666.
19 For the mononuclear Ni model complexes, see for example: (*a*) S. Fox, Y. Wang, A. Silver and M. Millar, *J. Am. Chem. Soc.*, 1990, **112**, 3218–3220; (*b*) H. J. Krüger, G. Peng and R. H. Holm, *Inorg. Chem.*, 1991, **30**, 734–742; (*c*) N. Baidya, M. M. Olmstead, J. P. Whitehead, C. Bagyinka, M. J. Maroney and P. K. Mascharak, *Inorg. Chem.*, 1992, **31**, 3612–3615; (*d*) C. A. Marganian, H. Vazir, N. Baidya, M. M. Olmstead and P. K. Mascharak, *J. Am. Chem. Soc.*, 1995, **117**, 1584–1594; (*e*) C.-H. Lai, J. H. Reibenspies and M. Y. Darensbourg, *Chem. Commun.*, 1999, 2473–2474; (*f*) D. Sellmann, F. Geipel and M. Moll, *Angew. Chem., Int. Ed.*, 2000, **39**, 561–563; (*g*) D. Sellmann, R. Prakash and F. W. Heinemann, *Eur. J. Inorg. Chem.*, 2004, 1847–1867; (*h*) C.-M. Lee, C.-H. Chen, S.-C. Ke, G.-H. Lee and W.-F. Liaw, *J. Am. Chem. Soc.*, 2004, **126**, 8406–8412; (*i*) C.-M. Lee, T.-W. Chiou, H.-H. Chen, C.-Y. Chiang, T.-S. Kuo and W.-F. Liaw, *Inorg. Chem.*, 2007, **46**, 8913–8923; (*j*) H. M. Alvarez, M. Krawiec, B. T. Donovan-Merkert, M. Fouzi and D. Rabinovich, *Inorg. Chem.*, 2001, **40**, 5736–5737; (*k*) E. Bouwman and J. Reedijk, *Coord. Chem. Rev.*, 2005, **249**, 1555–1581.
20 For the mononuclear Fe model complexes, see for example: (*a*) H.-F. Hsu, S. A. Koch, C. V. Popescu and E. Münck, *J. Am. Chem. Soc.*, 1997, **119**, 8371–8372; (*b*) C.-H. Lai, W.-Z. Lee, M. L. Miller, J. H. Reibenspies, D. J. Darensbourg and M. Y. Darensbourg, *J. Am. Chem. Soc.*, 1998, **120**, 10103–10114; (*c*) S. C. Davies, D. L. Hughes, R. L. Richards and J. R. Sanders, *Chem. Commun.*, 1998, 2699–2700; (*d*) A. C. Moreland and T. B. Rauchfuss, *Inorg. Chem.*, 2000, **39**, 3029–3036; (*e*) C. M. Whaley, T. B. Rauchfuss and S. R. Wilson, *Inorg. Chem.*, 2009, **48**, 4462–4469; (*f*) J. Jiang and S. A. Koch, *Angew. Chem., Int. Ed.*, 2001, **40**, 2629–2631; (*g*) D. Sellmann, F. Geipel and F. W. Heinemann, *Chem.–Eur. J.*, 2002, **8**, 958–966; (*h*) C.-H. Chen, Y.-S. Chang, C.-Y. Yang, T.-N. Chen, C.-M. Lee and W.-F. Liaw, *Dalton Trans.*, 2004, 137–143; (*i*) R. M. Henry, R. K. Shoemaker, R. H. Newell, G. M. Jacobsen, D. L. DuBois and M. R. DuBois, *Organometallics*, 2005, **24**, 2481–2491.
21 For the heteronuclear Ni/Fe model complexes, see for example: (*a*) F. Osterloh, W. Saak, D. Haase and S. Pohl, *Chem. Commun.*, 1997, 979–980; (*b*) D. Sellmann, F. Geipel, F. Lauderbach and F. W. Heinemann, *Angew. Chem., Int. Ed.*, 2002, **41**, 632–635; (*c*) M. C. Smith, J. E. Barclay, S. P. Cramer, S. C. Davies, W.-W. Gu, D. L. Hughes, S. Longhurst and D. J. Evans, *J. Chem. Soc., Dalton Trans.*, 2002, 2641–2647; (*d*) Z. Li, Y. Ohki and K. Tatsumi, *J. Am. Chem. Soc.*, 2005, **127**, 8950–8951; (*e*) P. A. Stenson, A. Marin-Becerra, C. Wilson, A. J. Blake, J. McMaster and M. Schroder, *Chem. Commun.*, 2006, 317–319; (*f*) Y. Ohki, K. Yasumura, K. Kuge, S. Tanino, M. Ando, Z. L. Li and K. Tatsumi, *Proc. Natl. Acad. Sci. U. S. A.*, 2008, **105**, 7652–7657; (*g*) W. Zhu, A. C. Marr, Q. Wang, F. Neese, D. J. E. Spencer, A. J. Blake, P. A. Cooke, C. Wilson and M. Schröder, *Proc. Natl. Acad. Sci. U. S. A.*, 2005, **102**, 18280–18285; (*h*) B. E. Barton, C. M. Whaley, T. B. Rauchfuss and D. L. Gray, *J. Am. Chem. Soc.*, 2009, **131**, 6942–6943; (*i*) J. Jiang, M. Maruani, J. Solaimanzadeh, W. Lo, S. A. Koch and M. Millar, *Inorg. Chem.*, 2009, **48**, 6359–6361; (*j*) C. Tard and C. J. Pickett, *Chem. Rev.*, 2009, **109**, 2245–2274; (*k*) Y. Ohki, K. Yasumura, M. Ando, S. Shimokata and K. Tatsumi, *Proc. Natl. Acad. Sci. U. S. A.*, 2010, **107**, 3994–3997; (*l*) Y. Ohki and K. Tatsumi, *Eur. J. Inorg. Chem.*, 2011, 973–985.
22 J. England, R. Gondhia, L. Bigorra-Lopez, A. R. Petersen, A. J. P. White and G. J. P. Britovsek, *Dalton Trans.*, 2009, 5319–5334.
23 J. H. Worrell, J. J. Genova and T. D. BuBois, *J. Inorg. Nucl. Chem.*, 1978, **40**, 441–446.
24 M. Mosimann, S.-X. Liu, G. Labat, A. Neels and S. Decurtins, *Inorg. Chim. Acta*, 2007, **360**, 3848–3854.
25 T. Pandiyan, S. Bernès and C. D. De Bazúa, *Acta Crystallogr., Sect. C: Cryst. Struct. Commun.*, 1999, **55**, 318–320.
26 D. Seyferth, R. S. Henderson and L.-C. Song, *J. Organomet. Chem.*, 1980, **192**, C1–C24.
27 Q. Wang, J. E. Barclay, A. J. Blake, E. S. Davies, D. J. Evans, A. C. Marr, E. J. L. McInnes, J. McMaster, C. Wilson and M. Schröder, *Chem.–Eur. J.*, 2004, **10**, 3384–3396.
28 D. Sellmann, F. Lauderbach and F. W. Heinemann, *Eur. J. Inorg. Chem.*, 2005, 371–377.
29 M.-C. Chalbot, A. M. Mills, A. L. Spek, G. J. Long and E. Bouwman, *Eur. J. Inorg. Chem.*, 2003, 453–457.
30 (*a*) A. Patra, S. Sarka, M. G. B. Drew, E. Zangrando and P. Chattopadhyay, *Polyhedron*, 2009, **28**, 1261–1264; (*b*) J. Becher, A. Hazell, C. J. McKenzie and C. Vestergaard, *Polyhedron*, 2000, **19**, 665–672.
31 M. G. B. Drew, D. A. Rice and K. M. Richards, *J. Chem. Soc., Dalton Trans.*, 1980, 2503–2508.
32 M. Y. Darensbourg, I. Font, D. K. Mills, M. Pala and J. H. Reibenspies, *Inorg. Chem.*, 1992, **31**, 4965–4971.
33 N. de Vries and J. Reedijk, *Inorg. Chem.*, 1991, **30**, 3700–3703.
34 V. V. Pavlishchuk, S. V. Kolotilov, A. W. Addison, R. J. Butcher and E. Sinn, *J. Chem. Soc., Dalton Trans.*, 2000, 335–341.
35 S. Karmakar, S. B. Choudhury, D. Ray and A. Chakravorty, *Polyhedron*, 1993, **12**, 291–299.

36 S. B. Choudhury, D. Ray and A. Chakravorty, *J. Chem. Soc., Dalton Trans.*, 1992, 107–112.
37 D. C. Goodman, T. Tuntulani, P. J. Farmer, M. Y. Darensbourg and J. H. Reibenspies, *Angew. Chem., Int. Ed. Engl.*, 1993, **32**, 116–119.
38 T. Yamamura, M. Tadokoro, M. Hamaguchi and R. Kuroda, *Chem. Lett.*, 1989, 1481–1484.
39 D. K. Mills, J. H. Reibenspies and M. Y. Darensbourg, *Inorg. Chem.*, 1990, **29**, 4364–4366.
40 B. Adhikary, S. Liu and C. R. Lucas, *Inorg. Chem.*, 1993, **32**, 5957–5962.
41 T. Pandiyan, V. M. Consuelo-Estrada, R. Moreno-Esparza and L. Ruiz-Ramírez, *Inorg. Chim. Acta*, 2003, **343**, 79–89.
42 C. M. Thomas, O. Rüdiger, T. Liu, C. E. Carson, M. B. Hall and M. Y. Darensbourg, *Organometallics*, 2007, **26**, 3976–3984.
43 J.-F. Capon, F. Gloaguen, P. Schollhammer and J. Talarmin, *J. Electroanal. Chem.*, 2004, **566**, 241–247.
44 L.-C. Song, L.-X. Wang, B.-S. Yin, Y.-L. Li, X.-G. Zhang, Y.-W. Zhang, X. Luo and Q.-M. Hu, *Eur. J. Inorg. Chem.*, 2008, 291–297.
45 H.-J. Krüger and R. H. Holm, *J. Am. Chem. Soc.*, 1990, **112**, 2955–2963.
46 L.-C. Song, Z.-Y. Yang, H.-Z. Bian, Y. Liu, H.-T. Wang, X.-F. Liu and Q.-M. Hu, *Organometallics*, 2005, **24**, 6126–6235.
47 F. Gloaguen, J. D. Lawrence, M. Schmidt, S. R. Wilson and T. B. Rauchfuss, *J. Am. Chem. Soc.*, 2001, **123**, 12518–12527.
48 B. E. Barton, C. M. Whaley, T. B. Rauchfuss and D. L. Gray, *J. Am. Chem. Soc.*, 2009, **131**, 6942–6943.
49 S. Canaguier, M. Field, Y. Oudart, J. Pécaut, M. Fontecave and V. Artero, *Chem. Commun.*, 2010, **46**, 5876–5878.
50 E. Barton and T. B. Rauchfuss, *J. Am. Chem. Soc.*, 2010, **132**, 14877–14885.
51 D. Seyferth, R. S. Henderson and L.-C. Song, *Organometallics*, 1982, **1**, 125–133.
52 E. Block, V. Eswarakrishnan, M. Gernon, G. Ofori-Okai, C. Saha, K. Tang and J. Zubieta, *J. Am. Chem. Soc.*, 1989, **111**, 658–665.
53 *CrystalClear and CrystalStructure*, Rigaku and Rigaku Americas, The Woodlands, TX, 2007.
54 G. M. Sheldrick, *SHELXS-97, Program for solution of crystal structures*, University of Göttingen, Germany, 1997.
55 G. M. Sheldrick, *SHELXL-97, Program for refinement of crystal structures*, University of Göttingen, Germany, 1997.

